

Analysis of a High-Performance C/A-Code GPS Receiver in Kinematic Mode

M. E. CANNON and G. LACHAPELLE

The University of Calgary, Calgary, Canada

Received January 1992

Revised June 1992

ABSTRACT

The results of a land semikinematic or stop-and-go test, conducted under normal operational conditions to assess the performance of a high-accuracy and multipath-resistant new C/A-code receiver technology, are presented. This type of test was selected to provide an accurate assesment of both the carrier phase and code data under static and kinematic conditions. The control points determined with the phase data are in agreement at the centimeter level with the values determined by a conventional GPS survey. The double-difference code residuals, which are affected by measuring noise and multipath, were found to behave in a quasi-random manner, with an estimated standard deviation of 50 cm. The effective multipath rejection characteristic of the receiver is attributed to the use of a narrow correlator spacing in the code tracking loops. Kinematic positioning tests based on code and carrier phase-smoothed code measurements using the between-receiver single-difference technique resulted in 1 m and 50 cm RMS accuracies, respectively, in each of the three coordinates. These accurate results will assist in the effective implementation of rapid carrier phase ambiguity resolution techniques for both the static and kinematic cases.

INTRODUCTION

In mid-1991, a new C/A-code GPS receiver technology was unveiled by NovAtel Communications, Ltd. [1]. One of the many unique characteristics of this receiver is a 10 cm C/A-code measuring noise level, i.e., one order of magnitude better than any other C/A-code receiver technology currently on the market. Such a high accuracy is important for solving the carrrier phase ambiguities rapidly, either in static or kinematic mode, and exploiting the millimeter accuracy level provided by carrier phase measurements. Another unique feature of this new technology is the optional use of narrow correlator spacing in the C/A-code tracking loops to reject multipath interference more effectively [2]. The 10-channel, 2/3-length board unit is designed to fit in a PC slot. Figure 1 shows a Grid 1535 EXP laptop containing one of the units used for the test, together with two antennas, one fitted with a 37 cm diameter choke ring ground plane to reduce multipath effects.

In the summer of 1991, the authors undertook the task of assessing this receiver for static and kinematic applications using software developed at The



Fig. 1 -GRID 1535 EXP Laptop Containing GPSCard™ and Antennas, With and Without Choke Ring Ground Plane

University of Calgary. Early static, two receivers/one antenna tests conducted in August 1991 confirmed the 10 cm CA-code measuring noise level claimed by the manufacturer in the absence of multipath [3]. The advantage of a two receivers/one antenna test is to isolate the uncorrelated code noise of the two receivers from the single antenna multipath, which cancels out in the differencing process. In real applications, however, multipath at both antennas will be uncorrelated and, as in the case of receiver noise, will be amplified in the differencing process. Thus the major question arising from the above two receivers/one antenna test is whether, under operational conditions, multipath is at such a level as to prevent the user from exploiting fully the 10 cm CA-code accuracy for quasi-instantaneous carrier phase ambiguity resolution. Previous experience has shown that C/A-code multipath effects on standard receivers can reach amplitudes of 10 to 20 m [4].

This paper investigates the performance of code and carrier phase measurements in both the static and kinematic environments, under normal operational multipath conditions, using semikinematic, i.e., stop-and-go, tests. The advantage of the semikinematic approach is the ability to control externally the accuracy achieved by the unit being assessed by stopping at precise control points along the kinematic trajectory. The sensitivity of the receiver to multipath is investigated by comparing results obtained with and without choke ring ground planes and using narrow versus wide correlator spacing.

-FIELD TESTS

The semikinematic tests reported in this paper were conducted in December 1991 and consisted of three differential GPS surveys, two of which were on the Kananaskis test range established by The University of Calgary in the Kananaskis Country. The third test, conducted with a wide correlator spacing

on the code tracking loops, took place between a few known points near Calgary. The system configurations and satellite geometry in terms of GDOP, HDOP, and VDOP are given for each test in Table 1. The Kananaskis test range, which is shown in Figure 2, consists of control points at a 1 km spacing along a stretch of road running in a north-south direction. For each point shown in Figure 2, there are in fact two control points, East (E) and West (W), one for each side of the road. The road segment used includes a forested and mountainous area that limits the satellite visibility to 10-20 deg elevation in several directions. Prototype choke ring ground planes were made specifically for the antennas by EM Technologies, Inc., of Fredericton, New Brunswick. Each ring is made of aluminum, and has a diameter of 37 cm and a weight of 10 kg. Three receiver units were used during the test, one at the monitor station and two on the rover, a Plymouth Minivan.

At each control point, for tests #1 and #3, the vehicle was brought to a stop, the antenna was moved to the control point using a bipod, and a few minutes of observations were made. The operating conditions during test #1 were far from optimal. Gusty winds of up to 100 km/h were frequent, causing vibrations on the bipod fitted with the 10 kg choke ring ground plane. Semikinematic test #2 was conducted at the same time as test #1 using another receiver mounted on the vehicle. At each control point, the antenna of this receiver

Table I-GPS System Configurations

Test	Choke Rings	Correlator Spacing'	GDOP	HDOP	VDOP
Semikinematic #1 ^b	Monitor & rover	Narrow	2.047	1.1-2.6	1.4-3.1
Semikinematic #2 ^b	Monitor only	Narrow	same as Test # 1		
Semikinematic #3	None	Wide	2.3-2.4	1.2-1.0	1.7-1.8

^aSee [2] for details.

^bKinematic tests #1 and #2 were carried out simultaneously using two receivers on the vehicle.

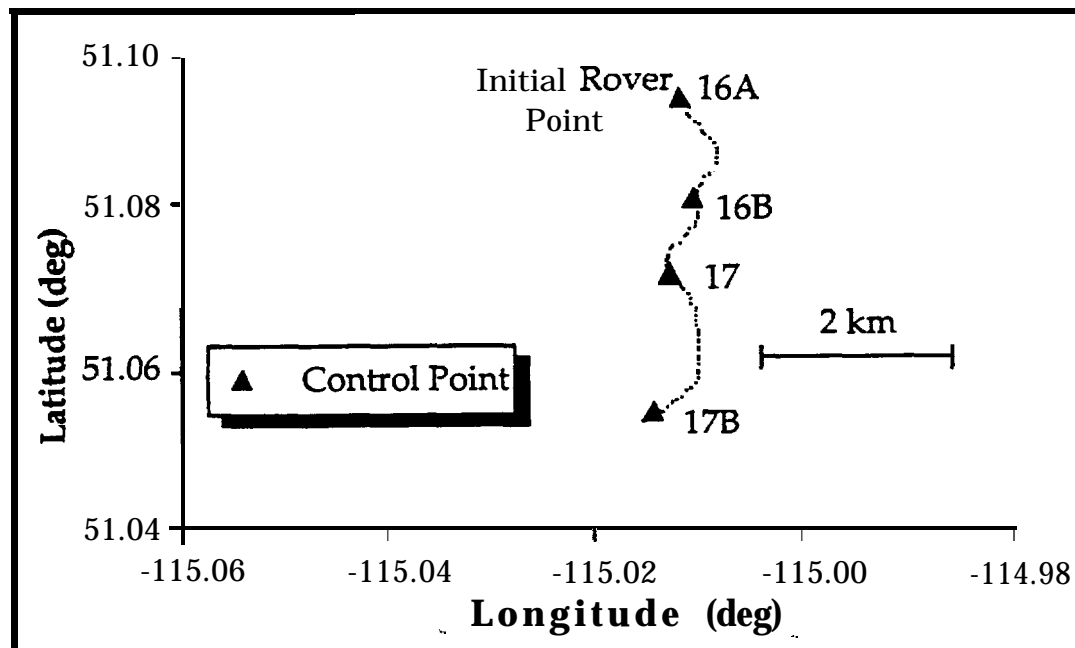


Fig. 2--University of Calgary GPS Test Range in Kananaskis Country

was left on the vehicle. This test was conducted to assess the code accuracy when no choke ring ground plane is used. Between control points, the vehicle reached speeds of 75 km/h.

The relative three-dimensional coordinates of the control points were established a few years ago using a conventional static differential GPS survey, and are accurate to a few centimeters. This test range has previously been used to test various receivers and software packages [5, 61. Station IGA(West) was used as the monitor and station IGA(East) as the initial station occupied by the rover in static mode for the initial ambiguity resolution, as shown in Figure 2. The maximum distance between the monitor and the vehicle was less than 5 km. The differential effects of orbital and atmospheric errors are therefore negligible in this case.

The satellite geometry was generally suboptimal. During the tests, five satellites were available simultaneously with an elevation ≥ 7.5 deg. Satellites with such low elevation angles are usually not used for high-accuracy positioning for a variety of reasons, including multipath. The GDOP varied between 2.0 and 4.7. The satellite elevations during semikinematic tests #1 and #2 are given in Table 2, in addition to the epochs at which cycle slips occurred. SV 23, a high satellite free of cycle slips, was used as the base satellite for all computations involving double differences. Over 90 percent of the cycle slips detected during test #2 occurred at nearly the same time as those which occurred during test #1, indicating that the causes were more than likely external to the receiver. Indeed, in the case of SV 6, the cycle slips occurred when the line of sight was grazing the tree tops. Tests #1 and #2 lasted about 50 min. Some 9 min of data could not be used in the middle of the test because of a drop to three satellites at one station, caused by signal masking. This left some 41 min or 2500 epochs of data collected on four or five satellites. The data was collected at a rate of 1 Hz.

In the case of test #2, the absence of a ground plane at the mobile receiver installed on the vehicle's roof did not result in more frequent cycle slips. This shows that the carrier phase tracking loops of the receiver are relatively stable in such a high-multipath environment.

SEMIKINEMATIC SURVEY WITH CARRIER PHASE OBSERVATIONS

This analysis was conducted to assess the performance of the receiver's raw carrier phase measurements for centimeter-level accuracy positioning. The software package SEMIKIN, developed at The University of Calgary and suc-

Table 2-Satellites Tracked and Cycle Slips Detected-Semikinematic Test #1

s v s	Elevation	Cycle Slips Detected (GPS epoch in second of week)
23 (base satellite)	68-86 deg	No cycle slips
6	14-8 deg	495368,495379,495703,496369, 96549,497233,497263,497347, 497563, 497989,498043
11	23-45 deg	495973,497089
17	52-28 deg	497593
21	43-68 deg	495247,495799,495829,497849, 497857.498169

cessfully tested with many other geodetic receivers [5,6], was used to process the data collected during test #1. SEMIKIN uses satellite-receiver double differences which, for short monitor-mobile distances, reduce to

$$\nabla\Delta\Phi = \nabla\Delta\rho + \lambda\nabla\Delta N + \epsilon\nabla\Delta(\Phi) \quad (1)$$

where Δ is the satellite-receiver double difference; Φ is the carrier phase in meters; $\rho = \|\mathbf{r} - \mathbf{R}\|$, \mathbf{r} being the computed position vector of the satellite using broadcast or post-mission ephemerides, and \mathbf{R} being the unknown position vector of the receiver; λ is the wavelength; ΔN is the double-difference carrier phase ambiguity, which is an integer number of cycles by definition; and $\epsilon\nabla\Delta(\Phi)$ is the carrier phase measurement noise and multipath. A Kalman filter is used to process the kinematic part of the survey, while a batch least-squares method is used during the short stops at the control points. The initial ambiguities are determined as integer numbers during the static initialization and are subsequently held fixed until a cycle slip is detected. In this mode of operation, a new static initialization is required to maintain centimeter-level accuracies if the number of cycle-slip-free satellites falls below four at any one point in time. Otherwise, the cycle slip is fixed using remaining cycle-slip-free observations.

The results of this semikinematic test are summarized in Table 3. The differences between the previously surveyed coordinates and the semikinematic results are shown. These vary between -6 and 3 cm, and are consistent with the accuracy of the control points and that expected of the current semikinematic survey technologies. In the latter case, errors include receiver noise, carrier phase multipath, the effect of suboptimal satellite geometry, and antenna centering errors. These results, which are in agreement with those obtained on the same test range with other geodetic receivers, are satisfactory and demonstrate high-quality raw carrier phase measurements.

The results also indicate that, between control points, the carrier phase-derived kinematic positions are accurate to the centimeter level. These accurate positions will be used in subsequent sections to assess the accuracy of code and carrier phase-smoothed code measurements under multipath conditions.

CODE MULTIPATH ANALYSIS IN KINEMATIC MODE

The use of the centimeter-level, carrier phase-based, semikinematic results described in the previous section makes this analysis straightforward. Code

Table 3-Results of Semikinematic Survey

Station	Control Points-Semikinematic Coordinates		
	Latitude	Longitude	Height
16AW (Monitor)	N/A	N/A	N/A
16AE (Ambiguity resolution through static initialization)	N/A	N/A	N/A
16BW	-4.0 cm	1.6 cm	-0.1 cm
17W	3.1	0.0	-3.3
17BE	0.6	1.9	1.4
17E	1.9	-6.4	0.8
16AE	-1.2	-5.4	-3.6

and carrier double differences, which are free from satellite and receiver clock errors, are compared as follows:

$$\delta = \nabla\Delta p - \nabla A @ \quad (2)$$

where p is the code measurement in meters. Over monitor-remote distances of less than 10 km, differential orbital and atmospheric effects are negligible. This leaves code and carrier noise and multipath. Since the combined effect of carrier noise and multipath is usually less than a few centimeters, we can assume that the above difference is due mostly to code noise and multipath. The two receivers/single antenna test conducted previously with these receivers confirmed a C/A-code noise level of 10 cm in the absence of multipath [3].

Code and carrier observations were recorded every s during the tests. Statistical averaging of the above yields

$$\delta_{\text{mean}} = [\Sigma(\Delta\nabla p_{C/A} - \Delta\nabla\Phi)]/n \quad (3)$$

$$\text{RMS}(\Delta\nabla p_{C/A}) = \sigma(\Delta\nabla p_{C/A}) = \{[\Sigma(\Delta\nabla p_{C/A} - \Delta\nabla\Phi)^2]/(n - 1)\}^{1/2}, \quad (4)$$

where the variance $\sigma^2(\Delta\nabla p_{C/A})$ consists of the sum of the receiver noise $\sigma^2(\Delta\nabla p_{\text{rx}(C/A)})$ and the multipath noise $\sigma^2(\Delta\nabla p_{\text{mult}(C/A)})$:

$$\sigma^2(\Delta\nabla p_{C/A}) = \sigma^2(\Delta\nabla p_{\text{rx}(C/A)}) + \sigma^2(\Delta\nabla p_{\text{mult}(C/A)}). \quad (5)$$

In equation (5), we have assumed that the multipath behaves in a random manner with a zero mean over a sufficiently long period of time. In our case,

$$\sigma(\Delta\nabla p_{\text{rx}(C/A)}) = 2\sigma(p_{\text{rx}(C/A)}) = 20 \text{ cm} \quad (6)$$

and

$$\sigma(\Delta\nabla p_{\text{mult}(C/A)}) = [\sigma^2(\Delta\nabla p_{C/A}) - (20 \text{ cm})^2]^{1/2} \quad (7)$$

Typical differences (6) between code and carrier phase double differences for tests #1 and #2 are shown in Figures 3 through 6. The reason for the 9 min data gaps between epochs 496500 and 497050 has been discussed earlier. The results are also summarized in Tables 4 and 5, which give the δ_{mean} and $\text{RMS}(\Delta\nabla p_{C/A})$ values for the double differences observed along the trajectory in both the kinematic and static modes. The mean differences between double-difference code and carrier do not exceed 10 cm, except for one pair, indicating that the multipath which is not rejected by the narrow correlator spacing tends to be generally random, justifying the statistical derivation presented above. The RMS values range from 49 to 79 cm in the case of test #1 (Table 4), where choke rings were used both at the monitor and at the remote. The corresponding values in the case of test #2 (Table 5) are 60 and 139 cm. An examination of the results plotted in Figures 3 through 6 reveals that large differences occur immediately after cycle slips. This is because the correlator spacing on the code tracking loops widens immediately after losses of lock, resulting in higher noise and a lower multipath rejection capability. To verify this, the RMS values were recalculated while excluding the first 90 s of data after each loss of phase lock, this being the estimated time delay required for the receiver tracking loops to reach their full performance level. These values, which are given in the last columns of Tables 4 and 5, range from 28 to 66 cm in the case of test #1, and from 35 to 72 cm in the case of test #2. The random effect of

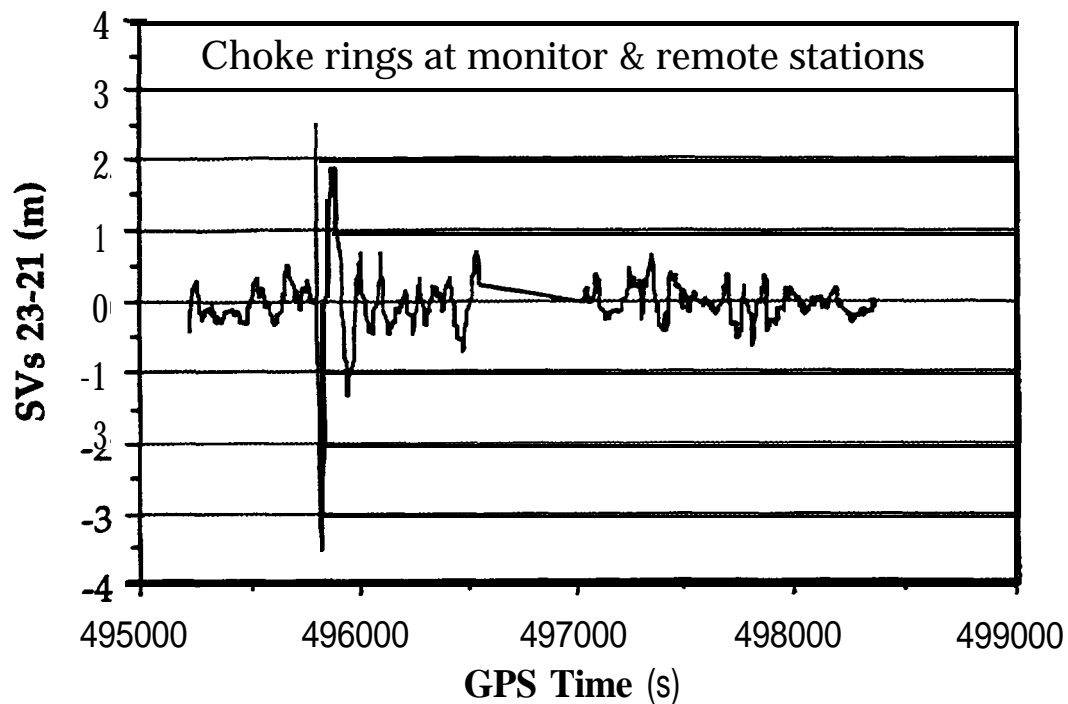


Fig. 3-Double-Difference Code Minus Double-Difference Carrier Phase for SVs 23-21, Test #1, Using a Narrow Correlator Spacing in the Code Tracking Loops

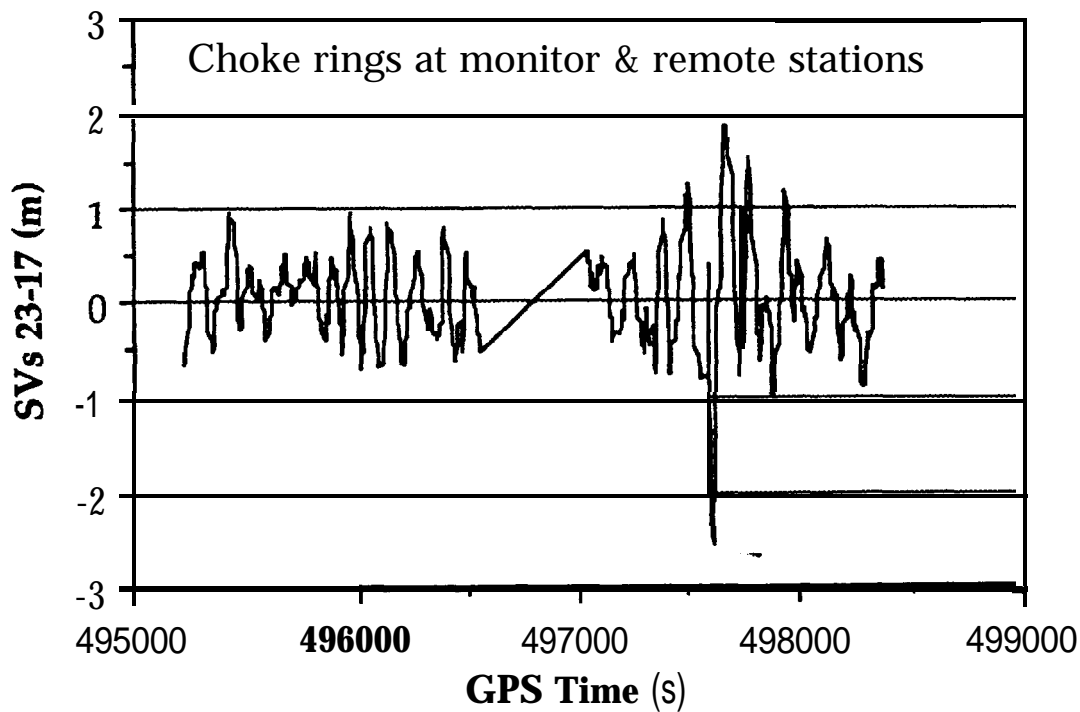


Fig. 1-Double-Difference Code Minus Double-Difference Carrier Phase for SVs 23-17, Test #1, Using a Narrow Correlator Spacing in the Code Tracking Loops

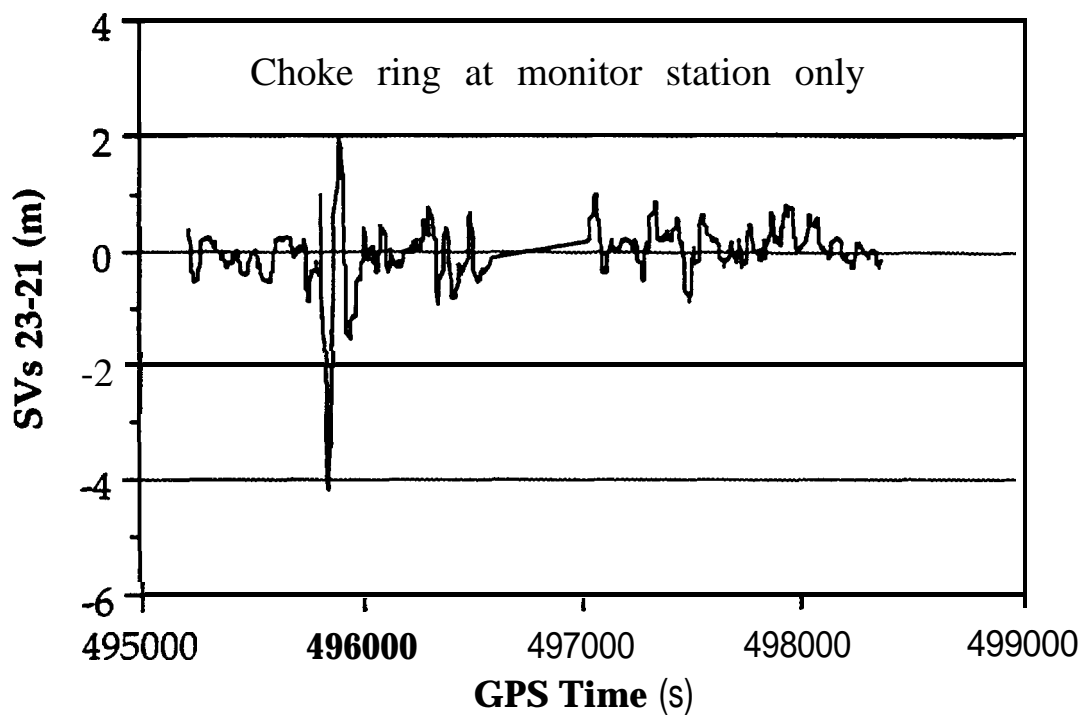


Fig. 5-Double-Difference Code Minus Double-Difference Carrier Phase for SVs 23-21, Test #2, Using a Narrow Correlator Spacing in the Code Tracking Loops

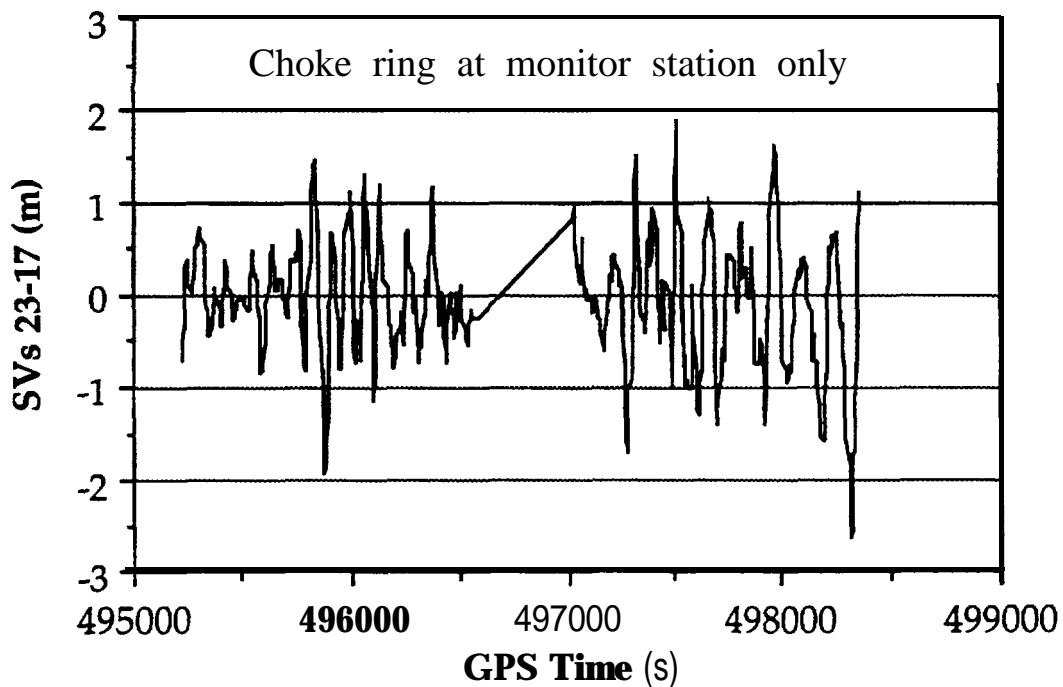


Fig. 6-Double-Difference Code Minus Double-Difference Carrier Phase for SVs 23-17, Test #2, Using a Narrow Correlator Spacing in the Code Tracking Loops

Table 4-Code Multipath Analysis: Double-Difference Code versus Double-Difference Carrier Phase (choke ring ground planes at both monitor and remote)

SVs ($\nabla\Delta$)	δ_{mean}	RMS($\Delta\nabla P_{C/A}$)	RMS($\Delta\nabla P_{C/A}$) ^a
23-6	- 8.0 cm	79 cm	66 cm
23-11	- 13.9	68	35
23-17	3.9	56	45
23-21	- 6.5	49	28

^aExcluding 90 s of data after each loss of phase lock.

Table 5-Code Multipath Analysis: Double-Difference Code versus Double-Difference Carrier Phase (choke ring ground plane at monitor only)

SVs ($\nabla\Delta$)	δ_{mean}	RMS($\Delta\nabla P_{C/A}$)	RMS($\Delta\nabla P_{C/A}$) ^a
23-6	9.3 cm	139 cm	72 cm
23-11	- 18.9	58	52
23-17	-8.1	65	68
23-21	-2.4	60	35

^aExcluding 90 s of data after each loss of phase lock.

multipath $\sigma(\Delta\nabla p_{\text{mult}(C/A)})$ on double-difference code can now be estimated easily using equation (7); it ranges from 20 to 70 cm. The corresponding effect on undifferenced code measurements is therefore 10 to 35 cm.

The use of a choke ring at the remote installed on the vehicle's roof, a relatively high-multipath environment, does not improve the results substantially. This is attributed to the high performance of the narrow correlator spacing used on the code tracking loops. This fact is well illustrated in Figures 7 and 8, which show typical results from test #3 when a wide correlator spacing was used. The code multipath reaches several meters, especially under static conditions. There is a strong correlation between multipath signature and vehicle speed. The higher the velocity, the more random multipath generally becomes. This phenomenon is well known for any propagated signal with a relatively small λ . The code multipath effects shown in Figures 7 and 8 would be those expected from a standard C/A-code receiver. A comparison of those figures with Figures 5 and 6 shows the improvement when using the narrow correlator spacing.

The results shown in Figures 3 through 6 and Tables 4 and 5 include the data collected in both the kinematic and static modes. A comparative analysis of the static and kinematic data collected during tests #1 and #2 shows that the standard deviations obtained during the kinematic parts of the tests were lower by 10-20 cm than those obtained during the static parts of the tests. This is consistent with our earlier statement regarding the randomness of multipath in kinematic mode.

CODE AND CARRIER PHASE-SMOOTHED CODE KINEMATIC POSITIONING

The kinematic positioning performance of the unit was also assessed using successively code-only and carrier phase-smoothed code measurements in differential mode using C³NAV (Combination of Code and Carrier for Navigation). This is a software package, developed by the authors, that uses between-

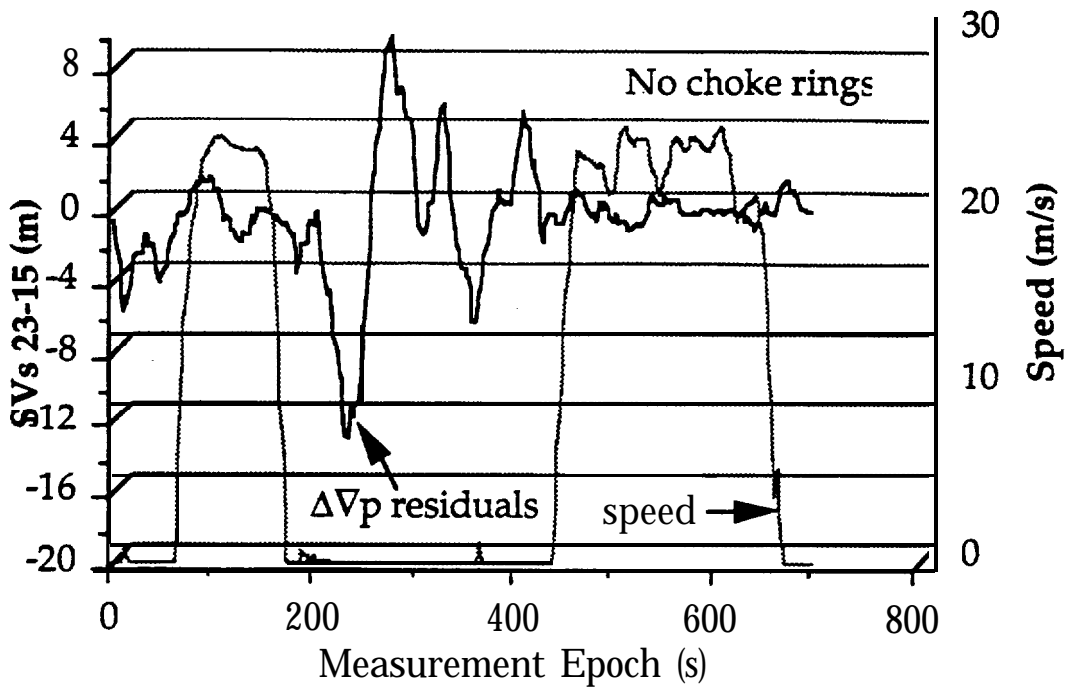


Fig. 7-Double-Difference Code Minus Double-Difference Carrier Phase for SVs 23-15, Test #3, Using a Wide Correlator Spacing in the Code Tracking Loops

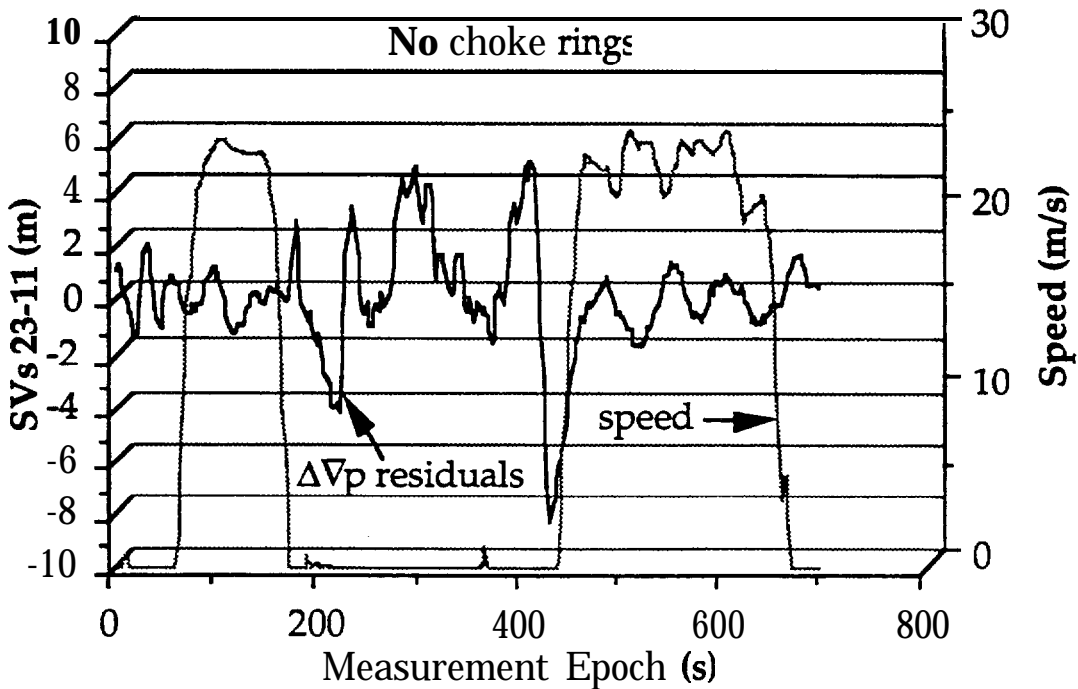


Fig. 8-Double-Difference Code Minus Double-Difference Carrier Phase for SVs 23-11, Test #3, Using a Wide Correlator Spacing in the Code Tracking Loops

receivers single differences, and is also suitable for real-time applications using a low data transmission rate. The pseudorange single difference between receivers can be written, for a short monitor-remote distance, as

$$A_p = \Delta\rho - c\Delta dT + \epsilon(\Delta p), \tag{8}$$

where ΔdT is the relative receiver clock. The error term $\epsilon(\Delta p)$ is not reduced by differentiation, but is increased because of the amplification of $\epsilon\Delta(p_{rx})$ by a factor of $\sqrt{12}$ since the $\epsilon(p_{rx})$'s are uncorrelated between receivers.

The carrier phase-smoothed code method uses pseudoranges observed at the same time as carrier phase measurements to estimate the carrier ambiguity with an accuracy of one to several cycles, depending on the accuracy of the pseudoranges [7]. Since the accuracy of pseudoranges $\sigma(\Delta\nabla p_{C/A})$ is generally worse than the one cycle level, a recursive filter that progressively increases the weight on Φ is used. In the approach described in [8], the phase-smoothed pseudorange \hat{P}_k at time k is

$$\hat{P}_k = W_{P_k}P_k + W_{\Phi_k} \{ \hat{P}_{k-1} + (\Phi_k - \Phi_{k-1}) \} \tag{9}$$

with initial conditions

$$\hat{P}_1 = P_1 \{ W_{P_1} = 1.0, W_{\Phi_1} = 1.0 - w_{p.,} = 0.0 \} \tag{10}$$

where P_k is the raw pseudorange at k , W_p is the weight assigned to the pseudorange, and W_Φ is the weight assigned to the carrier phase observation. We also have the conditions

$$W_{P_k} = W_{P_{k-1}} - 0.01, \text{ e.g., } 0.01 \leq W_{P_k} \leq 1.00 \tag{11}$$

$$W_{\Phi_k} = W_{\Phi_{k-1}} + 0.01, \text{ e.g., } 0.00 \leq W_{\Phi_k} \leq 1.00 \tag{12}$$

$$\sigma(\hat{P}_k) = f(\sigma_{P_k}, \text{multipath}). \tag{13}$$

The use of single-frequency C/A-code measurements has led to the following improvement ratio between raw and phase-smoothed pseudoranges [9]:

$$\sigma(P_k)/\sigma(\hat{P}_k) \approx 1.5 \text{ to } 3. \tag{14}$$

This translates typically into an RMS accuracy of 2-3 m in each of the coordinates when using code measurements accurate to 1-2 m [8].

To increase the reliability and level of robustness of this method under field conditions, to deal effectively with code/carrier divergence, and to limit the effects of wrong initial ambiguities and/or undetected cycle slips, parallel filters with frequent reinitialization can be used [4]; this method is also known as ramping. Parallel filters or ramps are reset at every n epochs, e.g., 100 to 500. A filter is used during a specific interval, e.g., $100 \leq n \leq 500$ in the present case. The interval is tuned as a function of parameters such as multipath. This approach has been implemented in C³NAV. In the present case, the differentially corrected positions of the rover were calculated in post-mission, and an update rate of 1 s was used. Any effect of Selective Availability would therefore be negligible.

In view of the above advantages, the carrier phase-smoothed pseudorange method remains a strong candidate for resolving carrier phase ambiguities in the present case. Its combination with an ambiguity search method, such as

the least-squares search and/or the ambiguity function method, may result in an accuracy near or at the one-cycle level when using the new C/A-code technology referred to above.

The C³NAV results obtained with the kinematic data collected during test #1 are shown in Figure 9 for the code-only data and in Figure 10 for the carrier phase-smoothed code. The test statistics are summarized in Table 6. As stated previously, the control points against which the C³NAV results are compared are the centimeter-level positions derived by SEMIKIN using carrier phase measurements with static initialization. The RMS agreement for any one coordinate component is usually well within the 1 m level in the case of code-only results and at the 50 cm level in the case of carrier phase-smoothed results. The contributing errors consist of code noise and multipath, receiver clock errors, and error amplification due to the satellite geometry. The 1 m threshold is usually exceeded only for a short period of time after a loss of phase lock, for the reasons stated earlier. The relative improvement when using carrier phase-smoothed pseudoranges is of the order of 2, well within the anticipated range of 1.5-3. An actual real-time differential kinematic test conducted using code measurements confirmed the 1 m accuracy level obtained herein [10].

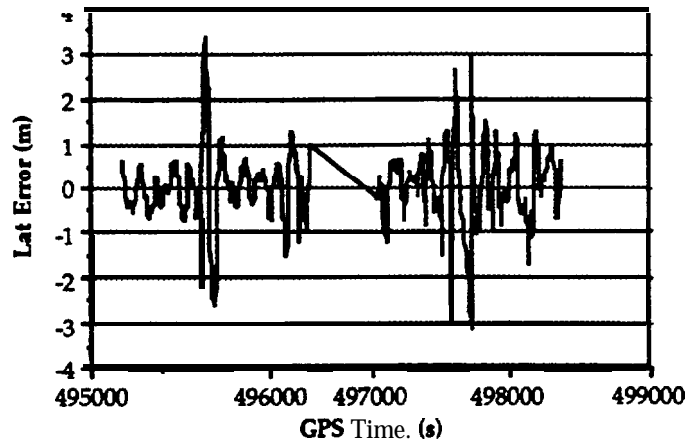
These results are considered fully satisfactory, considering the fact that the satellite geometry was suboptimal, with only five satellites available, one of these at a low elevation of 8 deg. The receiver clock error contribution appears to have little adverse effect on the accuracy. The carrier phase-smoothed solution, which is accurate to the 50 cm level, is satisfactory for a wide variety of kinematic applications. In addition, it constitutes an excellent approximate solution to determine the carrier phase ambiguities within one cycle on the fly using an ambiguity search technique [11, 12]. The relatively small initial search cube implied by the carrier phase-smoothed solution should enable one to determine the ambiguities in real time using portable commercial PCs.

CONCLUSIONS

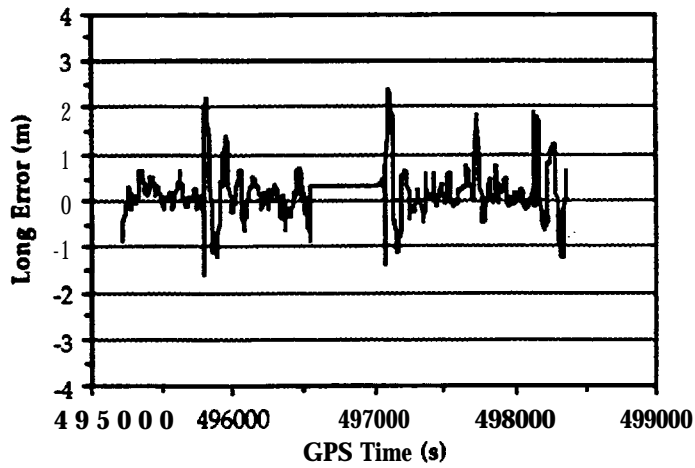
The land semikinematic test results reported herein show that:

- 1) The raw carrier phase measurements of the new C/A-code receiver technology tested deliver a level of performance similar to that of other geodetic receivers, based on the centimeter level accuracy obtained during the semikinematic survey.
- 2) The effect of multipath on double-difference code measurements, using a narrow correlator spacing in the code tracking loops and under the operational conditions encountered during the test, is at the 50 cm RMS level, with or without the use of antenna ground planes, and in either the static or kinematic mode.
- 3) Single-difference positioning using code-only measurements is at the 1 m accuracy level, while the use of carrier phase-smoothed code results in a 50 cm accuracy level, in terms of RMS differences in each of the three coordinate components.

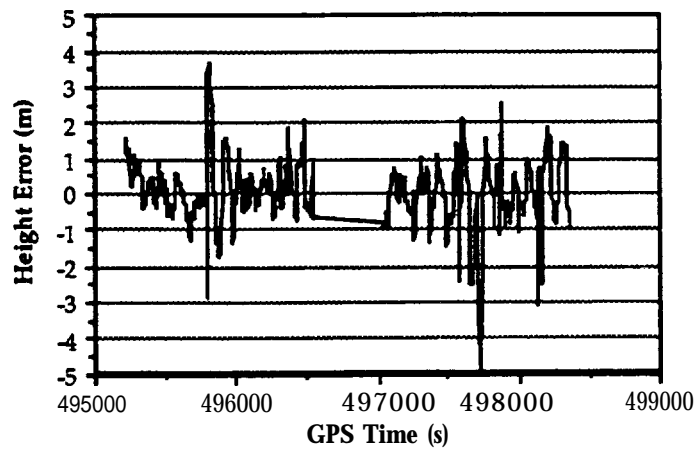
These tests were conducted under a suboptimal satellite geometry, with a GDOP of 4 and five satellites available, one of which was at an elevation angle



Latitude Component



Longitude Component



Height Component

Fig. 9-Between-Receiver Single-Difference Results in Kinematic Mode, Code-Only, Test #1

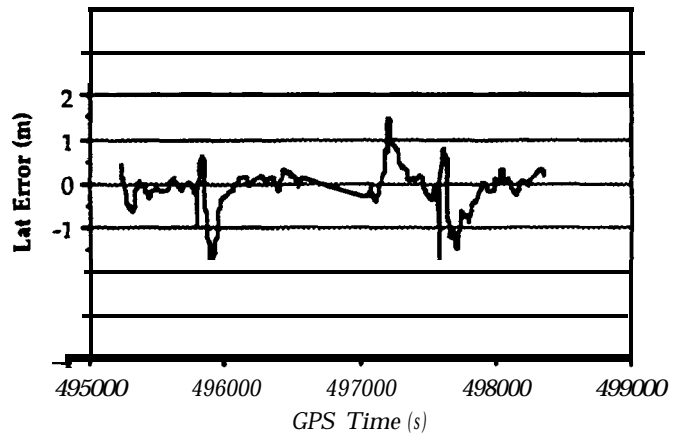
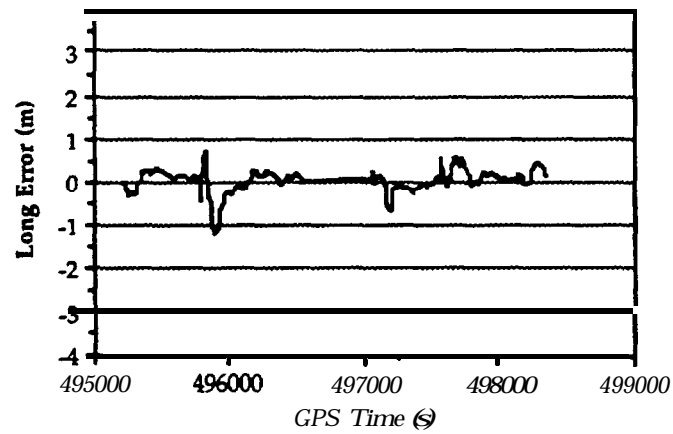
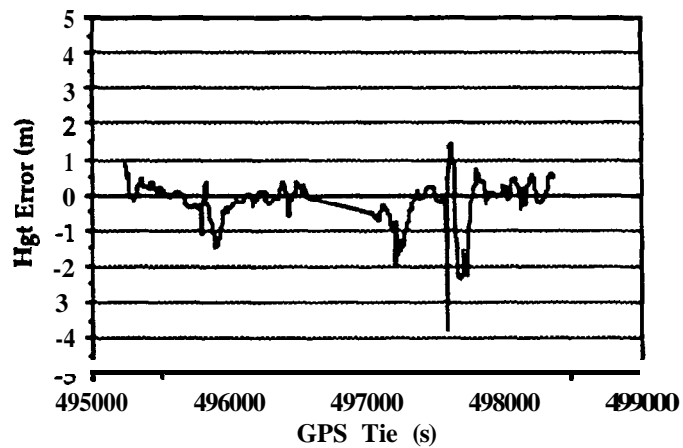
**Latitude Component****Longitude Component****Height Component**

Fig. 10-Between-Receiver Single-Difference Results in Kinematic Mode, Carrier Phase-Smoothed Code, Test #1

Table 6—Single-Difference Code and Carrier Phase-Smoothed Code Positioning

Coordinates	Code-only			Phase-Smoothed Code		
	δ_{mean}	δ_{max}	RMS	δ_{mean}	δ_{max}	RMS
Latitude	-0.02 m	3.45 m	0.82 m	-0.14 m	-2.54 m	0.50 m
Longitude	0.12	2.42	0.56	0.01	-1.26	0.28
Height	0.00	-5.49	0.99	-0.27	-3.88	0.66

of less than 10 deg for most of the test. The full constellation will likely improve the above positioning results.

The results show that even in the presence of cycle slips due to signal masking, a carrier phase-smoothed code solution constitutes a reliable and robust estimator for accuracies at the 50 cm level. This estimator will also provide an effective initial solution for the efficient implementation of on-the-fly ambiguity resolution techniques without static initialization, and for rapid ambiguity resolution in the case of static surveys. Both cases are currently being investigated, and initial results have been reported [11, 131].

Based on a paper presented at The Institute of Navigation National Technical Meeting, San Diego, California, January 1992.

REFERENCES

1. Fenton, P., Falkenberg, W., Ford, T., Ng, K., and Van Dierendonck, A. J., *NovAtel's GPS Receiver, the High Performance OEM Sensor of the Future*, Proceedings of GPS '91, The Institute of Navigation, pp. 49-58.
2. Van Dierendonck, A. J., Fenton, P., and Ford, T., *Theory and Performance of Narrow Correlator Spacing in a GPS Receiver*, in this issue of NAVIGATION.
3. Erickson, C., LaChapelle, G., and She, B. B., *Precise Rapid Static Surveys Using a Combination of Code and Carrier Measurements*, Proceedings of GPS '91, The Institute of Navigation, pp. 691-98.
4. LaChapelle, G., Falkenberg, W., Neufeldt, D., and Kielland, P., *Marine DGPS Using Code and Carrier in a Multipath Environment*, Proceedings of GPS '89, The Institute of Navigation, pp. 343-47.
5. Cannon, M. E., *High Accuracy GPS Semikinematic Positioning: Modelling and Results*, NAVIGATION, Journal of The Institute of Navigation, Vol. 37, No. 1, Spring 1990, pp. 53-64.
6. Cannon, M. E., LaChapelle, G., Ayers, H., and Schwarz, K. I., *A Comparison of SEMIKYN and KINSRVY for Kinematic Applications*, Proceedings of GPS '90, The Institute of Navigation, pp. 80-84.
7. Hatch, R., *The Synergism of GPS Code and Carrier Measurements*, Proceedings of the Third International Geodetic Symposium on Satellite Doppler Positioning, DMA/NGS, Washington, D.C., 1982, pp. 1213-32.
8. LaChapelle, G., Falkenberg, W., and Casey, M., *Use of Phase Data for Accurate Differential GPS Kinematic Positioning*, BULLETIN GEODESIQUE, Vol. 61, No. 4, 1987, pp. 367-77.
9. Goad, C. C., *Optimal Filtering of Pseudoranges and Phases from Single-Frequency GPS Receivers*, NAVIGATION, Journal of The Institute of Navigation, Vol. 37, No. 3, Fall 1990, pp. 249-62.
10. Falkenberg, W., Ford, T., Neumann, J., Fenton, P., Cannon, M. E., and LaChapelle, G., *Precise Real-Time Kinematic Differential GPS Using a Cellular Radio Modem*, Proceedings of PLANS '92, The Institute of Electrical and Electronics Engineers, New York, p. 391.

11. Lachapelle, G., Cannon, M. E., and Lu, G., ***Ambiguity Resolution on the Fly-A Comparison of P Code and High Performance CIA Code Receiver Technologies***, Proceedings of GPS '92, The Institute of Navigation, Alexandria, VA, September 1992.
12. Remondi, B. W., ***Kinematic GPS Results Without Static Initialization***, Proceedings of the 47th Annual Meeting, The Institute of Navigation, Washington, D.C., pp. 87-111.
13. Lachapelle, G., Cannon, M. E., Erickson, C., and Falkenberg, W., ***High Precision C/A Code Technology for Rapid Static GPS Surveys***, Proceedings of the Sixth International Geodetic Symposium on Satellite Positioning, Ohio State University, pp. 165-73.